

Dependence of *E. coli* Chemotaxis on CheB Phosphorylation *in Silico* and *in Vivo*

Lorenz Adlung¹
 Heidelberg University, Germany

Received 17.10.2011, accepted 30.11. 2011, published 03.12.2011

The protein CheB is an integral component of sensory adaptation in the chemotaxis system of *Escherichia coli*. It catalyzes demethylation of the chemoreceptors thereby opposing the effect of ligands on kinase activity. The kinase enhances the activity of the methyltransferase via phosphotransfer, thus creating a negative feedback. Although CheB phosphorylation depends on the receptor state, it is not essential for precise adaptation. Therefore, the feedback mechanism is proposed through modeling to compensate for protein fluctuations in the chemotaxis network.

Swarm plate assays revealed that chemotaxis performance in general was even more robust against deviations of single protein concentrations than predicted. However, phosphorylation deficient mutants of CheB still enabled an appropriate chemotaxis response as compared to wild type CheB. Furthermore, when simulations were recoded to include CheB phosphorylation, there was no effect on swarming.

Hence both, measured and calculated swarm efficiencies indicate that CheB phosphorylation does not improve robustness of chemotaxis against perturbations in protein levels.

1 Introduction

Thanks to pioneering work¹, bacterial chemotaxis became one of the most studied and well-documented systems in molecular biology. The machinery for cell motility senses and reacts upon temporal changes in chemoefactor concentrations. Signal transduction components are encoded by six essential genes: *cheA*, *cheB*, *cheR*, *cheW*, *cheY* and *cheZ*. Partially redundant² membrane-spanning receptors (e.g. Tar) transmit input cues from the periplasmic space to the cytoplasm (Fig. 1).

CheW acts as an adapter between receptors and the histidine kinase CheA, which catalyzes the transfer of phosphoryl groups from ATP to own histidine residues. The phosphoryl group is rapidly transferred to response regulators; in this case mainly CheY. The phosphorylated CheY (CheY-P) is released from the complex, diffuses and binds to flagellar motor switches. The rotary motors are embedded in the cell envelope³. As an output, CheY-P switches the flagellar rotation from counter-clockwise (CCW) to clockwise (CW)⁴, resulting in different swimming behavior of the cell. The phosphatase CheZ mediates turnover of chemotaxis response by dephosphorylation of CheY-P close to the receptors⁵. Evolved interactions between those molecular components ensure an optimal chemotaxis performance⁶. Attractant binding to the receptor inhibits kinase activity. Subsequently low CheY-P levels result in persistent counter-clockwise flagellar rotation and thence unchanged swimming direction of the cell. Repellents (or declining attractant concentrations) sensed by the receptor cause activation of CheA and induce phosphorylation of response regulator CheY. The flagellar rotation is shifted to clockwise and the cell starts "tumbling".

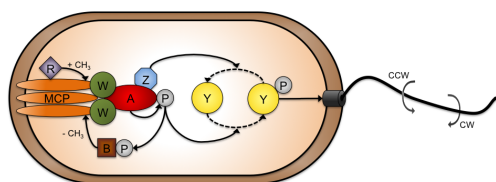


Figure 1: Schematic overview of the chemotaxis pathway. Components are abbreviated. For further details, refer to the text.

Driven by the molecular machinery, the microbe runs in favorable directions towards high concentrations of attractant and away from repellents. An amazing feature of the chemotaxis system is adaptation. This is the property to maintain sensitivity over a wide range of chemical stimuli. Even at saturating concentrations of attractants or repellents, the system returns gradually to pre-stimulus values, which means that kinase activity,

CheY-P level and motor bias adapt precisely to a certain steady state. Additionally, this ability seems to be robust against changes in concentrations of chemotaxis proteins. *E. coli* chemotaxis turned out to be a simple but well-adjusted system with robustness of adaptation precision through its network architecture⁷.

The molecular components which are responsible for adaptation are CheR and CheB. Methyltransferase CheR constitutively methylates specific receptors, i.e. methyl accepting chemotaxis proteins (MCP). Methylation increases receptor potential to stimulate kinase activity and decreases receptor affinity to attractants⁸. The reverse reaction is catalyzed by the methyl-erasing CheB. Concerning the structure, CheB consists of two domains connected by a short linker sequence. The regulatory N-terminus is homologous to CheY. Both proteins bind competitively to the P2 domain of CheA⁹ and can be phosphorylated by the activated kinase as response regulators. Phosphorylation at Asp56 leads to conformational changes of CheB¹⁰ and increases its affinity to the receptor cluster¹¹. However, N-terminal deletion mutants, which cannot be phosphorylated, still maintain chemotaxis ability and appropriate swimming behavior¹². The unphosphorylated N-terminal domain exerts an inhibition on the effector domain by partially occluding the active site of CheB. Kinetic analyses indicate nearly 100-fold increase of CheB methyl-erasing activity through relief of inhibition and stimulation of catalysis by phosphorylation¹³.

Receptors in the active state lead to autophosphorylation of CheA and phosphotransfer to CheB. Hence activated CheB catalyzes MCP demethylation and receptor activity diminishes. Interestingly, such a negative feedback loop is not essential for precise adaptation¹⁴. This raises the question of the exact role of CheB phosphorylation in the chemotaxis pathway. How does swarming performance of *E. coli* depend on the feedback via CheB? There are at least theoretical indications that CheB phosphorylation provides robustness, in terms of unaffected swarming performance, against varying chemotaxis protein concentrations¹⁵. Here, experiments and simulations were conducted to analyze the proposed function of the feedback loop. Swarm plate assays¹⁶ were combined with the use of *RapidCell*¹⁷, a multi-scale modeling software for swarming bacteria. Results suggest a new perspective on the methyl-erasing and its regulatory function.

2 Experiments and Simulations

The role of CheB phosphorylation was investigated *in vivo* via swarm plate assays. Ideal swarming conditions were determined including suitable induction levels for chemotaxis gene expression from plasmid. The knockout strain (Δ *cheB*) was transformed with a plasmid encoding either wild type CheB or one of the mutants CheB^{D56E} and CheBc. Those restore function to some degree. After titration, strains were co-transformed with another plasmid containing one of the other chemotaxis genes. The resulting swarming performances were evaluated referring to up-regulated

¹The theoretical work was done at BioQuant Institute, Im Neuenheimer Feld 267, 69120 Heidelberg, Germany and experiments were conducted at Zentrum für Molekulare Biologie der Universität Heidelberg, Im Neuenheimer Feld 282, 69120 Heidelberg, Germany. Corresponding email address: l.adlung@dkfz-heidelberg.de

protein levels of each CheA, CheR, CheW, CheY, CheZ and Tar. It was the aim to see whether wild type CheB phosphorylation provides additional robustness against over-expression of chemotaxis genes as compared to the deficient mutants. To study chemotaxis *in silico*, an equation representing CheB phosphorylation was integrated into the *RapidCell* program code. The software sources for input and output were refined. Simulated results were then compared to experimental observations.

2.1 CheB Titration

Wild type CheB or one of the two mutants, CheB^{D56E} and CheBc, were expressed from a plasmid in the $\Delta cheB$ strain. They were tested for complementation to chromosome-encoded CheB in wild type strains. The mutant CheB^{D56E} cannot be phosphorylated due to the point mutation and shows only a basal level of activity. The mutant CheBc lacks the N-terminal regulatory domain and the remaining catalytic domain with a short linker cannot interact suitably with the chemotaxis cluster. Corresponding genes were expressed from plasmids with an arabinose-inducible promoter.

E. coli requires a functional chemotaxis system to swarm on soft agar plates. The cells spread radially, because they form attractant gradients by metabolizing nutrients in the agar. Complementation CheB, CheB^{D56E} and CheBc in the $\Delta cheB$ strain affected swarming. Optimal swarming for CheB was obtained with 0.001 % arabinose. Swarm ring sizes changed with arabinose induction level and were compared to the wild type strain for calculation of relative chemotaxis efficiency. Protein amounts of all CheB variants were quantified with Western blots relative to CheB levels of the wild type strain.

The phosphorylation mutant was expressed at least two fold of wild type level to enable swarming (Fig. 2). Presumably, basal activity of CheB^{D56E} was insufficient for functionality of chemotaxis at wild type expression level. In contrast, strains expressing CheBc swarmed already if the mutant level averaged 20 % of wild type CheB (Fig. 2). Reported ten-fold increase in methyltransferase activity compared to unphosphorylated CheB¹³ would be reasonable in this case. CheBc represents the uninhibited state of CheB through relief of the regulatory domain. The methyltransferase without N-terminus is constitutively active and suspected to localize to polar receptors by direct interactions with the MCPs¹⁸. Huge amounts of CheBc would then result in permanent demethylation of receptors what directly promoted stimulation by attractants and improved chemotaxis performance. That is, why CheBc expressing strains swarmed better at high induction levels than those expressing wild type CheB under laboratory conditions. It remained unclear if swarm efficiency would diminish for higher CheBc levels or if swarming would reach a steady state through saturation of net demethylation.

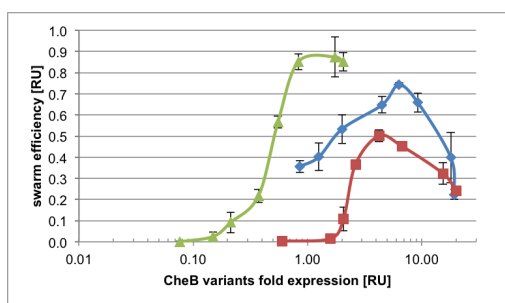


Figure 2: Dependence of swarm efficiency on expression levels of CheB variants. Blue line with diamonds: $\Delta cheB$ + CheB, red line with squares: $\Delta cheB$ + CheB^{D56E}, green line with triangles: $\Delta cheB$ + CheBc. Standard deviations are given by error bars, n=3.

The curve for swarm efficiency with increasing protein levels of CheB was less steep as compared to the mutants (Fig. 2). The smooth gradient of the graph hinted at a more balanced mediation of swarming via CheB and some feature of robustness contrary to high sensitivity of CheB^{D56E} and CheBc.

2.2 Chemotaxis Performance of CheB Variants

The next aim was to see if CheB phosphorylation provides robustness of the chemotaxis system against single protein fluctuations. Robustness

means stable output (i.e. constant swarming behavior) despite perturbations (i.e. various expression levels). Therefore, plasmid-encoded chemotaxis proteins were simultaneously expressed with CheB, CheB^{D56E} or CheBc from respective plasmids in the *cheB* knock-out strain. CheB variants were always induced with the preliminarily obtained optimal concentration of 0.001 % arabinose (see 2.1). The expression of the other chemotaxis genes was always induced with increasing levels of IPTG.

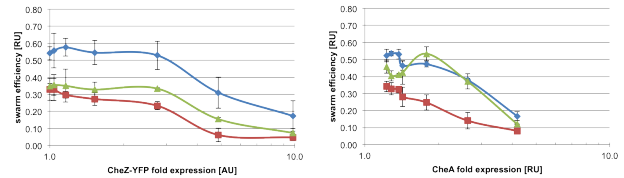


Figure 3: Chemotaxis performance for over-expression of CheZ-YFP (left panel) and CheA (right panel). Blue line with diamonds: $\Delta cheB$ + CheB, red line with squares: $\Delta cheB$ + CheB^{D56E}, green line with triangles: $\Delta cheB$ + CheBc. Standard deviations are given by error bars, n=6 (CheZ-YFP) or n=7 (CheA). Quantifications of CheZ-YFP via flow cytometry normalized to lowest induction level. Quantifications of CheA via Western blots referring to wild type.

Chemotaxis in general was unexpectedly robust against up-regulation of the referring proteins, here fused to the yellow fluorescent protein (YFP). Only high over-expression of e.g. CheZ-YFP led to reduction of swarming ability (Fig. 3). Wild type CheB and its phosphorylation was not observed to counter-balance this effect. Reduction of swarming was similar for wild type CheB and the mutants. Advantages resulted exclusively from 0.001 % arabinose induction but not from phosphorylation of wild type CheB. Results for CheW looked quite similar (data not shown).

In case of CheA, the native protein was studied since YFP fusions to CheA exhibit no appropriate function¹¹. Expression levels were not as high as for the other chemotaxis proteins. The CheBc mutant strain mediated better swarming than wild type CheB within a narrow range around two-fold wild type expression (Fig. 3). This observation was consistent with explanations from the literature: While CheB interacts via its N-terminus with the P2 domain of CheA¹⁹, the methyltransferase activity is inhibited. Due to the lack of the regulatory domain, CheBc is not hampered, and increased CheA levels do not have a direct influence on CheBc activity. Consequently, robustness of chemotaxis is provided by CheBc against particular up-regulation of CheA.

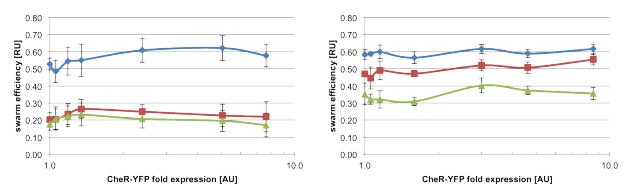


Figure 4: Swarming robustness against CheR over-expression in the $\Delta cheRB$ strain (left panel) and the $\Delta cheB$ strain (right panel). Blue line with diamonds: $\Delta che(R)B$ + CheB, red line with squares: $\Delta che(R)B$ + CheB^{D56E}, green line with triangles: $\Delta che(R)B$ + CheBc. Standard deviations are given by error bars, n=6 ($\Delta cheRB$) or n=4 ($\Delta cheB$). Quantifications via flow cytometry, normalized to lowest induction level.

For the Tar receptor, expression levels were also very low (data not shown). A distinction between wild type CheB and CheBc was again hardly possible and CheB^{D56E} performance was just slightly worse. This further supported the hypothesis that chemotaxis performance does not benefit from the phosphorylation of wild type CheB in terms of robustness.

Methyltransferase CheR was investigated as C-terminal YFP fusion in a $\Delta cheRB$ strain and the $\Delta cheB$ strain. Chemotaxis behavior was robust over a broad range of CheR-YFP expression in the double knock-out strain (Fig. 4). Strikingly, complemented wild type CheB showed advanced swarming in comparison to CheB mutants. During same experiments in the $\Delta cheB$ background, the mutants tended to be more motile (Fig. 4). A considerable difference is the presence of native CheR in the $\Delta cheB$ strain,

albeit in low concentrations²⁰. An interaction between CheR-YFP from plasmid and chromosome-encoded CheR was assumed to cause changes in swarming. A direct interaction between native CheR and the CheB mutants is unlikely¹¹. Such an eminent disparity between swarming performances in $\Delta cheB$ strain and double knock-out strain expressing CheB mutants was unprecedented and remains to be resolved.

Theoretical considerations could facilitate investigation of the chemotaxis system and enhance our understanding. An auspicious software for large-scale simulations of swarming bacteria is *RapidCell*¹⁷. So far, *RapidCell* was lacking an equation for the CheB phosphorylation. In this work, *RapidCell* was advanced for theoretical studies of the CheB feedback loop to enable comparison between mentioned experiments and those simulations.

2.3 Software Refinement and Analysis

Receptor methylation and demethylation is described in *RapidCell* by an ordinary differential equation (ODE). The program operated with phosphorylated CheB (CheBP) as a static parameter assuming CheB activity is not changing over time. Such a lack of CheB regulation obviously led to worse swarming behavior as indicated *in vivo* by the phosphorylation mutant CheB^{D56E}. With an equation for CheB phosphorylation, the negative feedback loop for regulation of CheB activity was introduced into the model. CheBP became a dynamic variable, which was updated for every time step in response to other network properties. The ODE was adopted¹⁵:

$$\partial_t \text{CheBP} = k_{\text{CheBP}} \cdot \text{CheAP} \cdot (\text{CheB}^T - \text{CheBP}) - \gamma_{\text{CheBP}} \cdot \text{CheBP} \quad (1)$$

The change of CheBP concentration over time was dependent on the following two parameters:

- (I) k_{CheBP} , the rate of phosphotransfer from autophosphorylated CheA (CheAP) to CheB. Phosphorylation was proportional to CheAP and the concentration of unphosphorylated CheB, i.e. total amount of CheB (CheB^T) minus CheBP.
- (II) γ_{CheBP} , the dephosphorylation rate of CheBP. This turnover was solely dependent on CheBP because it is autocatalytic.

The changing CheBP concentrations directly influenced methylation state, which in turn altered the free-energy offset in the model. This had an impact on the system activity CheAP that fed back to CheBP values. These regulations balanced the system's output. Moreover, the feedback loop brought the model in a closer agreement to experimental data (Fig. 5).

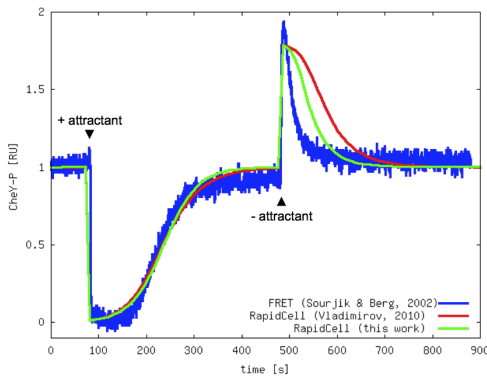


Figure 5: Comparison of two *RapidCell* versions with experimental data. The change of phosphorylated CheY (CheY-P) in a single cell is plotted with time. The *RapidCell* version of this work includes CheB phosphorylation. Both simulations with identical settings.

Response of phosphorylated CheY (CheY-P) was measured via Förster Resonance Energy Transfer (FRET) after adding and removing attractant. Active CheB is required to return CheY-P to steady state. This CheB-dependent adaptation was fitted to the experimental results. The parameters k_{CheBP} and CheB^T were refined to ensure a physiological amount of active CheBP. With the introduced phosphorylation equation, CheBP levels changed with CheAP. Theoretically, robustness is expected¹⁵ when:

$$\frac{\partial \text{CheBP}}{\partial \text{CheAP}} > 0 \quad (2)$$

is fulfilled. Similarly, robustness is expected at least against over-expression of CheY and CheZ. Equation 2 was true for the model that included CheBP regulation but not for the old version with only one static value for CheBP. These differences between the software versions did not become obvious for calculated swarming behavior (data not shown).

With over-expression of CheY-YFP, swarm efficiencies for all CheB variants diminished likewise (Fig. 6). The better wild type performance resulted again exclusively from the preliminary obtained optimal induction level. There was no additional robustness. This observation was in line with the simulation results (Fig. 6). CheB variants could not be discriminated.

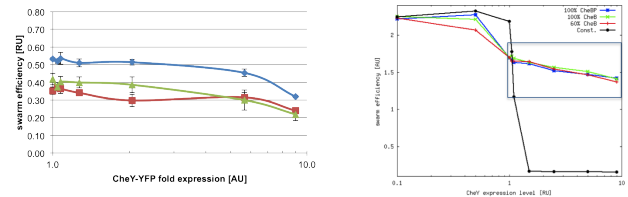


Figure 6: Swarm efficiencies for different CheY levels. Experiments with CheY-YFP in the $\Delta cheB$ strain expressing again different CheB variants (left panel) and referring simulations (right panel). Blue curve: software including CheB phosphorylation. Green curve: program lacking the equation. Red curve: simulation with only 60% CheB activity relative to wild type. Black graph: a calculation for another attractant gradient. Dark blue rectangle as a guide to the eye for experimentally determined expression range.

For CheY levels, a sensitive readout with steep input-output characteristics is known²¹. Small variations trigger large change in motor bias. The more CheY is present in the cell, the more likely it will be phosphorylated in competition with CheB. Phosphorylated CheY promotes tumbling. Hence, swarm efficiency was expected to drop when CheY gets out of its tight working range. This effect was tremendous for a constant activity gradient that was recommended for simulations of chemotaxis efficiency¹⁷. For gaussian gradient, simulated chemotaxis fitted swarm plate assay results. The impact of the applied attractant gradient in the model should be taken into further consideration since it dramatically altered the sensitivity of the system.

3 Conclusions

In summary, the smooth shape of the curve for wild type CheB during titration (Fig. 2) hinted at some impact of CheB phosphorylation on mediating chemotaxis performance. Those results suggest a regulatory function connected to the feedback loop. The over-expression studies (Fig. 3, Fig. 4) indicated that the robustness of chemotaxis performance in attractant gradients is not originating from CheB phosphorylation though the system exhibited high robustness in general. Predicted sensitivity of chemotaxis against protein up-regulation in some attractant gradients was contradictory (Fig. 6) to experiments.

On the other hand, the negative feedback loop definitely fine-tuned the system's response kinetics after removal of attractant (Fig. 5). Declining attractant concentrations have same effects on the system as increasing repellent gradients. Future approaches should therefore be addressed to repellent swarming where the impact of CheB phosphorylation could be more pronounced. Such experiments are more elaborate²². But to elucidate those mechanisms, it could be worthwhile shifting the focus to repellent taxis.

Quite often in biology, structure and function are intimately associated. However, many questions concerning the relation between architecture and function of biological graphs and their evolution remain elusive. Negative feedback loops represent a generic motif in molecular pathways. They define dynamic signaling properties. Dissecting the role of CheB phosphorylation in chemotaxis could add valuable information to our understanding of network building blocks in nature. Perspectively, one could then re-engineer the chemotaxis machinery, e.g. to enable deliberate drug delivery or to aid intervention of microbial spread.

4 Acknowledgements

The work could not have been done without the contributions of: Prof. Dr. Victor Sourjik, Dr. Sonja Schulmeister, Dr. Ilka Bischofs-Pfeifer, Dr. Nikita Vladimirov, Prof. Dr. Ursula Kummer, Dr. Sven Sahle and all members of the “Sourjik Lab”.

References

- [1] J Adler. Chemotaxis in bacteria. *Science*, 153(737):708–716, 1966.
- [2] I B Zhulin. The superfamily of chemotaxis transducers: from physiology to genomics and back. *Adv Microb Physiol*, 45:157–198, 2001.
- [3] H C Berg. The rotary motor of bacterial flagella. *Annu Rev Biochem*, 72:19–54, 2003.
- [4] U Alon, L Camarena, M G Surette, B Aguera y Arcas, Y Liu, S Leibler, and J B Stock. Response regulator output in bacterial chemotaxis. *EMBO J*, 17(15):4238–4248, 1998.
- [5] V Sourjik and H C Berg. Binding of the *Escherichia coli* response regulator CheY to its target measured *in vivo* by fluorescence resonance energy transfer. *Proc Natl Acad Sci U S A*, 99(20):12669–12674, 2002.
- [6] S Schulmeister, M Ruttorf, S Thiem, D Kentner, D Lebiecz, and V Sourjik. Protein exchange dynamics at chemoreceptor clusters in *Escherichia coli*. *Proc Natl Acad Sci U S A*, 105(17):6403–6408, 2008.
- [7] N Barkai and S Leibler. Robustness in simple biochemical networks. *Nature*, 387(6636):913–917, 1997.
- [8] K A Borkovich, L A Alex, and M I Simon. Attenuation of sensory receptor signaling by covalent modification. *Proc Natl Acad Sci U S A*, 89(15):6756–6760, 1992.
- [9] J Li, R V Swanson, M I Simon, and R M Weis. The response regulators CheB and CheY exhibit competitive binding to the kinase CheA. *Biochemistry*, 34(45):14626–14636, 1995.
- [10] S Djordjevic, P N Goudreau, Q Xu, A M Stock, and A H West. Structural basis for methyltransferase CheB regulation by a phosphorylation-activated domain. *Proc Natl Acad Sci U S A*, 95(4):1381–1386, 1998.
- [11] D Kentner and V Sourjik. Dynamic map of protein interactions in the *Escherichia coli* chemotaxis pathway. *Mol Syst Biol*, 5:238, 2009.
- [12] R C Stewart and F W Dahlquist. N-terminal half of CheB is involved in methyltransferase response to negative chemotactic stimuli in *Escherichia coli*. *J Bacteriol*, 170(12):5728–5738, 1988.
- [13] G S Anand and A M Stock. Kinetic basis for the stimulatory effect of phosphorylation on the methyltransferase activity of CheB. *Biochemistry*, 41(21):6752–6760, 2002.
- [14] U Alon, M G Surette, N Barkai, and S Leibler. Robustness in bacterial chemotaxis. *Nature*, 397(6715):168–171, 1999.
- [15] M Kollmann, L Lovdok, K Bartholome, J Timmer, and V Sourjik. Design principles of a bacterial signalling network. *Nature*, 438(7067):504–507, 2005.
- [16] N Vladimirov and V Sourjik. Chemotaxis: how bacteria use memory. *Biol Chem*, 390(11):1097–1104, 2009.
- [17] N Vladimirov, L Lovdok, D Lebiecz, and V Sourjik. Dependence of bacterial chemotaxis on gradient shape and adaptation rate. *PLoS Comput Biol*, 4(12):e1000242, 2008.
- [18] S Banno, D Shiomi, M Homma, and I Kawagishi. Targeting of the chemotaxis methyltransferase/deamidase CheB to the polar receptor-kinase cluster in an *Escherichia coli* cell. *Mol Microbiol*, 53(4):1051–1063, 2004.
- [19] A M Stock, D C Wylie, J M Mottonen, A N Lupas, E G Ninfa, A J Ninfa, C E Schutt, and J B Stock. Phosphoproteins involved in bacterial signal transduction. *Cold Spring Harb Symp Quant Biol*, 53 Pt 1:49–57, 1988.
- [20] M Li and G L Hazelbauer. Cellular stoichiometry of the components of the chemotaxis signaling complex. *J Bacteriol*, 186(12):3687–3694, 2004.
- [21] P Cluzel, M Surette, and S Leibler. An ultrasensitive bacterial motor revealed by monitoring signaling proteins in single cells. *Science*, 287(5458):1652–1655, 2000.
- [22] D L Englert, M D Manson, and A Jayaraman. Investigation of bacterial chemotaxis in flow-based microfluidic devices. *Nat Protoc*, 5(5):864–872, 2010.